Chemistry and Physics of Lipids 225 (2019) 104813

Contents lists available at ScienceDirect

Chemistry and Physics of Lipids

journal homepage: www.elsevier.com/locate/chemphyslip

Improved approach for comprehensive profiling of gangliosides and sulfatides in rat brain tissues by using UHPLC-Q-TOF-MS

Xiong-Yu Meng[a], Lee-Fong Yau[a], Hao Huang[a], Wai-Him Chan[a], Pei Luo[a], Li Chen[a], Tian-Tian Tong[a], Jia-Ning Mi[a], Zifeng Yang[a,b], Zhi-Hong Jiang[a], Jing-Rong Wang[a,*]

[a] State Key Laboratory of Quality Research in Chinese Medicine, Macau Institute for Applied Research in Medicine and Health, Macau University of Science and Technology, Taipa, Macau, China

[b] State Key Laboratory of Respiratory Disease, National Clinical Research Center for Respiratory Disease, Guangzhou Institute of Respiratory Health, the First Affiliated Hospital of Guangzhou Medical University, Guangzhou, Guangdong, 510120, China

ARTICLE INFO

Keywords:
Acidic glycosphingolipids (GSLs)
Gangliosides (GAs)
Sulfatides (STs)
Pre-fractionation
Rat brain
UHPLC-Q-TOF-MS

ABSTRACT

Gangliosides (GAs) and sulfatides (STs) are major acidic glycosphingolipids (GSLs) that are particularly abundant in the central nervous system and associated with substantial neurodegenerative diseases. In this study, we developed an improved approach for the comprehensive profiling of GAs and STs in rat brain tissues by adopting a pre-fractionation step before the LC–MS analysis. The pre-fractionation step allows the efficient enrichment of different types of acidic GSLs and the removal of high-abundance interferences, thereby greatly enhanced the detection sensitivity and accuracy of low-abundance acidic GSLs. By using this improved approach, a total of 340 acidic GSLs (from 281 compositions) were characterized in rat brain tissues, including 277 GAs (from 230 compositions) and 63 STs (from 51 compositions), among which 57 GAs and 14 STs were novel acidic GSLs that have not been reported previously. This study represented the most comprehensive profiling of acidic GSLs in rat brain tissues. The result of this study greatly enlarged our understanding of the structural diversity of natural acidic GSLs, and provided important chemical information for the exploration of biological function of acidic GSLs in the central nervous system.

1. Introduction

Glycosphingolipids (GSLs) are amphipathic molecules composed of a hydrophilic glycan chains linked to a hydrophobic ceramide moiety through a glycosidic linkage (Yu et al., 2009). Gangliosides (GAs) and sulfatides (STs) are two major acidic GSLs that contain negatively charged residues. GAs possess one or more sialic acids that are predominantly linked to the galactose residues, or a few that are linked to the inner N-acetylgalactosamine (GalNAc) residue (Yu et al., 2011). Core structures of GA can be additionally modified by O-acetylation (OAc) (Sonnino et al., 2007), fucosylation (Fuc), (Vukelic et al., 2006) and an/the attachment of GalNAc (Li, 2012). STs own a sulfated galactose and is possibly attached to a glucose residue (Eckhardt, 2008). Moreover, the ceramide moiety of both GAs and STs emerged with high heterogeneity in chain length, degree of unsaturation, and hydroxylation (Kolter et al., 2002; Wang et al., 2014; Huang et al., 2016; Mi et al., 2016a).

GAs and STs are particularly abundant in the central nervous system (CNS), but they are also ubiquitously found in other tissues, such as retina and kidney (Masson et al., 2015, Tian et al., 2017), as well as in body fluids, such as serum and milk (Yu et al., 2011; Rivas-Serna et al., 2015). Cellular GAs are implicated in many physiological and pathophysiological processes, such as cell growth, differentiation, embryogenesis, neurogenesis, and tumor progression (Kolter, 2012). More importantly, GAs are involved in many neurophysiological functions in the CNS, such as synaptic transmission, synaptogenesis, and neurogenesis. Therefore, they are associated with many neurodegenerative diseases, including Alzheimer's disease, Parkinson's diseases, and

Abbreviation: GSL, glycosphingolipid; GA, ganglioside; ST, sulfatide; OAc, O-acetylation; Fuc, fucosylation; GalNAc, *N-acetylgalactosamine*; SA, sialic acid; GM, monosialoganglioside GM1; GD, disialoganglioside GD; GT, trisialoganglioside GT; GQ, tetrasialoganglioside GQ; GP, pentasialoganglioside GP; UHPLC, Ultra-High Performance Liquid Chromatography; Q-TOF, Quandrupole-Time-of-Flight; MS, mass spectrometry; SPE, Solid Phase Extraction; RP, Reverse Phase; HILIC, hydrophilic interaction liquid chromatography

* Corresponding author at: State Key Laboratory of Quality Research in Chinese Medicine Macau Institute for Applied Research in Medicine and Health, Macau University of Science and Technology Taipa, Macau, China.

E-mail address: jrwang@must.edu.mo (J.-R. Wang).

https://doi.org/10.1016/j.chemphyslip.2019.104813
Received 29 June 2019; Received in revised form 5 August 2019; Accepted 20 August 2019
Available online 20 August 2019
0009-3084/

Huntington's disease (Yanagisawa, 2007; Kolter, 2012; Alpaugh et al., 2017). STs act as essential components of the myelin sheaths and are associated in protein trafficking, signal transduction, and neuronal cell differentiation (Han et al., 2003). For these reasons, there has been an increasing interest in acidic GSLs as biomarkers or therapeutic targets for CNS diseases (Wang et al., 2015; Li et al., 2018).

The biological function of acidic GSLs is largely determined by their structures. Therefore, it is pivotal to establish methods for the comprehensive characterization of acidic GSLs in biological samples. Among all currently employed methods, mass spectrometry (MS) is considered as one of the most reliable (Zamfir, 2014) tool for the structural analysis of acidic GSLs due to its high resolution, accuracy, and sensitivity (Mohammadi et al., 2016; Skraskova et al., 2016; Tian et al., 2017). To reduce ion-suppression from various interferences in complex biological samples, the coupling of MS with liquid chromatography (LC) has become the most conventional analysis strategy (Tonidandel and Seraglia, 2007). In recent years, there has been a breakthrough in the number of identified acidic GSLs. This was achieved by employing a reversed-phase (RP) column with the addition of formic acid in the mobile phase (Hu et al., 2017), and by using a hydrophilic interaction chromatography (HILIC) column with the optimization of pH value and buffer composition of mobile phase (Hajek et al., 2017).

Approximately 200 acidic GSLs have been identified from brain tissues to date (Sarbu et al., 2016). However, owing to the highly heterogeneous and diverse molecular structures of acidic GSLs, substantial acidic GSLs that may present as low abundance or trace species need to be explored. The challenges for the detection of low abundance acidic GSLs majorly arise from the ion-suppression of co-eluted species or non-target lipids. In addition, due to the structural complexity of acidic GSLs, the interfering signals among species with similar molecular weight can be quite serious, resulting in great difficulty in the differentiation of isobaric or isomeric acidic GSLs. Notably, the interfering signals derived from matrix, contaminants, and isomers may compromise the MS/MS spectra of acidic GSLs, thereby hindering the identification of acidic GSLs. To solve these problems, we herein developed a pre-fractionation procedure prior to LC–MS analysis of acidic GSLs. Then we characterized the acidic GSLs according to high-resolution MS and MS/MS data acquired from UHPLC-Q-TOF-MS. The characterizations were further supported by RP-LC the retention rule and confirmed with commercial standards.

2. Materials and methods

2.1. Materials and chemicals

Sep-Pak C_{18} cartridges (3cc, 500 mg, 37–55 μm) were purchased from Waters (Milford, MA, USA). Acidic GSL standards, including fucosylated GM1 (Fuc-GM1 (d18:1/18:0)), GD3 (d18:1/23:0), GT1b (d18:1/18:0), GQ1b (d18:1/18:0), and N-Octadecanoyl-sulfatides (ST (d18:1/18:0)) were purchased from Matreya LLC (State College, PA). Standards of GM1 (d18:1/18:0), GM2 (d18:1/18:0), GM3 (d18:1/18:0), GD1a (d18:1/18:0), GD1b (d18:1/18:0), and GD2 (d18:1/18:0) were purchased from Sigma-Aldrich (St. Louis, MO). Formic acid (HCOOH) of HPLC grade and ammonium formate (NH_4HCOO) of MS grade were purchased from Sigma-Aldrich (St. Louis, MO). Methanol (MeOH) of MS grade was purchased from J.T. Baker (Avantor Performance Materials, LLC. Center Calley, PA, USA). Chloroform ($CHCl_3$) of HPLC grade was purchased from RCI Labscan Limited (Bangkok, Thailand). Ultrapure water (18.2 MΩ) was prepared using a Milli-Q system (Millipore, MA, USA).

2.2. Animals

Sprague-Dawley (SD) rats (180–220 g), 6 males and 6 females, were purchased from Chinese University of Hong Kong. Animals were housed in cages with free access to food and water in a room on a 12 h light/dark cycle, and temperature was maintained at 20 ± 0.5 °C. All animal experiments were approved by the Division of Animal Control and Inspection, Department of Food and Animal Inspection and Control, Instituto para os Assuntos Cívicos e Municipais (IACM), Macao. Rat brain tissues were frozen in liquid nitrogen immediately after collection, and were stored at −80 °C until further analysis.

2.3. Extraction of acidic GSLs

Acidic GSLs were extracted from rat brain tissues on the basis of the method developed by Svennerholm & Fredman (Svennerholm, 1963; Svennerholm and Fredman, 1980) and Folch (Folch et al., 1957). Firstly, brain tissues were homogenized in 5-fold volume of PBS and washed twice with PBS; the homogenized sample was dispersed in 8-fold volume of PBS. Secondly, an aliquot of 100 μL of brain tissue homogenate and 4 mL of $CHCl_3$/MeOH (C/M; 2:1, v/v) were added into a 12 mL borosilicate glass tube. The sample mixture was agitated for 20 min in an orbital shaker at room temperature for total lipid extraction. In order to separate acidic GSLs from other lipids, 0.8 mL of water was added into the sample mixture, after which the mixture was vortexed for 5 min and centrifuged at 3000 rpm and 4 °C for 15 min. The upper phase was collected into a new 12 mL borosilicate glass tube. Then, 0.9 mL of MeOH and 0.8 mL of water were added to the lower $CHCl_3$ phase and vortexed for 5 min. The mixture was centrifuged at 3000 rpm and 4 °C for 15 min to separate the two phases. Finally, both upper phases that containing total acidic GSLs were pooled together and dried under gentle nitrogen stream. The dried residue was reconstituted in 100 μL of MeOH and centrifuged at 12,000 rpm and 4 °C for 5 min to precipitate residual proteins. The supernatant was collected and stored at −80 °C until the next step.

2.4. Pre-fractionation of extracted acidic GSLs

Prior to pre-fractionation, the C_{18} cartridge was pre-conditioned sequentially with 2 × 3 mL MeOH and 3 × 3 mL water. Next, 100 μL of acidic GSLs extract was loaded onto the C_{18} cartridge, and the flow-through was re-loaded onto the cartridge. The cartridge was washed with 3 mL of water to remove salt and other interferences. Then, acidic GSLs were eluted from the C_{18} cartridge with 20%, 40%, 50%, 70%, 75%, 80%, 85%, 90%, and 100% MeOH sequentially (3 mL for each gradient). Each 1 mL of the eluent was collected individually and examined using UHPLC-TOF MS. Eluents containing GSLs of the same type were combined to yield fractions that enrich GM, GD, GT, GQ, and GP respectively.

2.5. UHPLC-Q-TOF-MS conditions

Acidic GSLs analysis was performed according to the approach developed by Hu et al (Hu et al., 2017) with minor modification in our lab. The chromatographic separation was performed on an Agilent 1290 Infinity UHPLC system (Agilent Technologies, Santa Clara, CA, USA) with an Agilent Zorbax Eclipse Plus C_{18} column (100 × 2.1 mm, 1.8 μm). The mobile phase consisted of (A) H_2O and (B) MeOH, both containing 0.2% HCOOH and 10 mM NH_4HCOO. The linear gradient was as follows: 0–3 min, 80–85% B; 3–17 min, 85–100% B; 17–19 min, 100% B; 19–19.01 min, 100-80% B; 19.01–25 min, 80% B. The flow rate was 0.4 mL/min, the column temperature was controlled at 45 °C, and the injection volume was 10 μL. MS and MS/MS analysis was carried out on an Agilent ultrahigh definition (UHD) 6550 Q-TOF mass spectrometer (Agilent Technologies, Santa Clara, CA, USA) with a dual Agilent jet stream electrospray ionization (dAJS-ESI) source. The acquisition parameters for Q-TOF-MS detection were as follows: nebulizer pressure, 20 psi; sheath gas flow, 11 L/min; sheath gas temperature, 250 °C; drying gas flow, 14 L/min; drying gas temperature, 200 °C. MS spectra and MS/MS spectra were acquired in positive mode with the

mass range of *m/z* 500–3000 and *m/z 50*–3000, respectively. A reference solution was nebulized for continuous calibration using the reference masses of *m/z* 922.0098. Targeted MS/MS was acquired with the collision energy (CE) set at 15, 45, and 50 eV.

2.6. Nomenclature of acidic GSLs

Annotation of the glycan chain moiety of GAs is assigned according to the nomenclature system of Svennerholm (Svennerholm, 1963, Chester, 1998). First, the ganglio- series is denoted by the capital letter "G", followed by a capital letter designating the number of sialic acid (SA) ("M" = 1, "D" = 2, "T" = 3, "Q" = 4, "P" = 5). Then, the following Arabic number denotes the length of the sugar residues ("1″ = 4 sugars, "2″ = 3 sugars, "3″ = 2 sugars, "4″ = 1 sugar). Finally, the number of SA on the innermost galactose is designated by a lower-case letter ("a" = 1 SA, "b" = 2 SAs, "c" = 3 SAs"). Therefore, this can be exemplified by GQ1b, which has 4 SAs (Q), 4 sugar residues (1), and two of its four SAs on the innermost galactose (b). Furthermore, the glycan chain moiety of GAs can be modified by O-acetylation, fucosylation, and attachment of N-acetylgalactosamine, which are denoted as OAc, Fuc, and GalNAc, respectively.

Annotation of the ceramide moiety of GAs and STs are assigned according to the nomenclature system of LIPID MAPS (Lipidomics Gateway). Hydroxyl group number ("d" = 2 hydroxyl groups, "t" = 3 hydroxyl groups), carbon number (18), and double bond number (1) in the sphingoid backbone, and carbon number (16), and double bond number (0) in the N-acyl chain are denoted as (d18:1/16:0).

2.7. Establishment of personal database of acidic GSLs

Based on the LIPID MAPS information, which has recorded 1551 GAs and STs online (5 December 2018), a personal acidic GSLs database was established in the Agilent Mass Hunter Personal Compound Database and Library (PCDL) software. This PCDL included all biologically plausible acidic GSLs with ceramide carbon numbers that varied from 24 to 70, degrees of unsaturation that varied from 0 to 10, number of sialic acids that varied from 1 to 10, and all possible modifications, such as *O*-acetylation, fucosylation, sulfation and attachment of N-acetylgalactosamine.

2.8. Data processing

All data analysis was processed with Agilent Mass Hunter Qualitative Analysis B.07.00 software. Find by formula (FBF) algorithm was employed for mining acidic GSLs in rat brain tissues. The following matching criteria was set: our personal acidic GSLs database was imported as the formula source and a maximum of 5 possible matches were allowed per formula; mass tolerance was set as ± 15 ppm; proton (+H) and sodium (+Na) adducts in positive mode and charge state ranged from 1 to 3 were allowed for matching; the overall score (including mass score, isotope abundance score, and isotope spacing score) < 70 was set as the result filters.

3. Results

3.1. Pre-fractionation of acidic GSLs by using C_{18} cartridge

Eluents collected from C_{18} cartridge were analyzed by using UHPLC-Q-TOF-MS; acidic GSLs were combined by types. As a result, 5 fractions that respectively enriched GP (40% MeOH eluent), GQ and GT (50 to 70% MeOH eluent), GD (75 to 80% MeOH eluent), GM (85% MeOH eluent), as well as ST (90% MeOH eluent) were obtained. Of note, glycerophospholipids, the dominant contaminant in total acidic GSL extract, were mostly removed upon pre-fractionation (Fig. 1).

One of the significant benefits obtained from pre-fractionation is the resolving of co-eluted acidic GSLs that often interfere with each other in MS detection, especially when the co-eluted compounds are isobaric or isomeric species. Upon the resolving, mutual interference of the co-eluted species can be eliminated greatly, which subsequently led to a notable increase in signal-to-noise ratio (S/N) and a great improvement of mass accuracy. Such enhanced MS detection can provide crucial evidence for the identification of co-eluted species, especially low abundance species. For example, a pair of co-eluted species, GM1 (d20:1/18:1) (Cpd.**28**) and OAc-GQ1b (d20:1/20:2) (Cpd.**267**), were respectively separated into Fr. 4 and Fr. 3 upon pre-fractionation. This led to a 3-fold increase of the S/N of Cpd.**28** and about 80% increment of the S/N of Cpd.**267.** In addition, the mass accuracy of both compounds improved greatly due to the elimination of mutual interference, which facilitated reliable identification of these two acidic GSLs (Fig. 2A). By using similar approaches, a total of 22 pairs of co-eluted acidic GSLs were identified in the current study (Supporting information Table. S1).

Another noteworthy benefit with the pre-fractionation is the remarkably reduced ionization suppression arising from non-targeted lipids or matrix. The S/N and signal intensity of low-abundance acidic GSLs can increase dramatically due to the reduced ionization suppression. For instance, upon pre-fractionation, the S/N of GQ1b (d18:1/23:0) (Cpd.**246**) increased by about 7-fold, and the signal intensity was enhanced by approximately 4-fold (Fig. 2B). Therefore, pre-fractionation enabled the discovery of acidic GSLs that could not be detected by routine methodology, as exemplified by the identification of GT1b (d18:1/25:1) (Cpd.**218**) (Fig. 2C). By using this strategy, a total of 71 novel acidic GSLs were identified in the current study (Supporting information Table. S1).

3.2. Identification and characterization of acidic GSLs in rat brain tissues

3.2.1. Characterization of acidic GSLs based on high-resolution MS and MS/MS

3.2.1.1. Structural elucidation of GAs. On the basis of the high-resolution MS and MS/MS data, structures of GAs were characterized. This can be exemplified by the identification of Cpd.**242.** According to its $[M+2H]^{2+}$ ion at *m/z* 1210.5909, the molecule formula of Cpd.**242** was deduced as $C_{106}H_{182}N_6O_{55}$. MS/MS analysis of $[M+2H]^{2+}$ ion at *m/z* 1210.5909 provided characteristic fragments for the glycan chain and ceramide moiety, respectively. First, four consecutive 291 gaps from *m/z* 2420.1702 to *m/z* 2129.0739, *m/z* 1837.9804, *m/z* 1546.8981 and *m/z* 1255.7990 were observed as a result of the sequential loss of four sialic acid groups. This information suggested that Cpd.**242** possesses four sialic acids, and therefore belongs to the GQ type. Second, one 162 gap from *m/z* 1255.7990 to *m/z* 1093.7462, one 203 gap from *m/z* 1093.7462 to *m/z* 890.6717, and two 162 gaps from *m/z* 890.6717 to *m/z* 728.5937, and then *m/z* 566.5548 were observed, indicating the existence of a sugar chain of Hex-HexNAc-Hex-Hex on Cpd.**242**. Third, the ions at *m/z* 583.1974 ($[2*NeuAc+H]^+$), *m/z* 745.2600 ($[2*NeuAc+Hex+H]^+$) and *m/z* 948.3331 ($[2*NeuAc+Hex+HexNAc+H]^+$) supported that two tandem sialic acids are attached on a Hex unit. Hence, Cpd.**242** was assigned as a GQ1b (Fig. 3A). The structure of Cpd.**242** was further elucidated based on the fragments arising from ceramide moiety. Briefly, ions at *m/z* 548.5479 ($[M\text{-glycan chain-}H_2O+H]^+$), *m/z* 530.5381 ($[M\text{-glycan chain-}2*H_2O+H]^+$) and *m/z* 518.5340 ($[M\text{-glycan chain-}H_2O-HCOH+H]^+$) suggested the presence of two hydroxyl groups in ceramide moiety of Cer (d36:1). Then, the ions at *m/z* 282.2796 ($[d18:1\text{-}H_2O+H]^+$), *m/z* 264.2682 ($[d18:1\text{-}2*H_2O+H]^+$) and *m/z* 252.2571 ($[d18:1\text{-}H_2O-HCOH+H]^+$) indicated the presence of a d18:1 sphingoid backbone. Based on the aforementioned evidence, Cpd.**242** was characterized as GQ1b (d18:1/18:0) (Fig. 3B).

3.2.1.2. Structural elucidation of modified GAs. Substantial modifications of GA by O-acetylation, fucosylation, and attachment of N-acetylgalactosamine were found in rat brain tissues. For O-

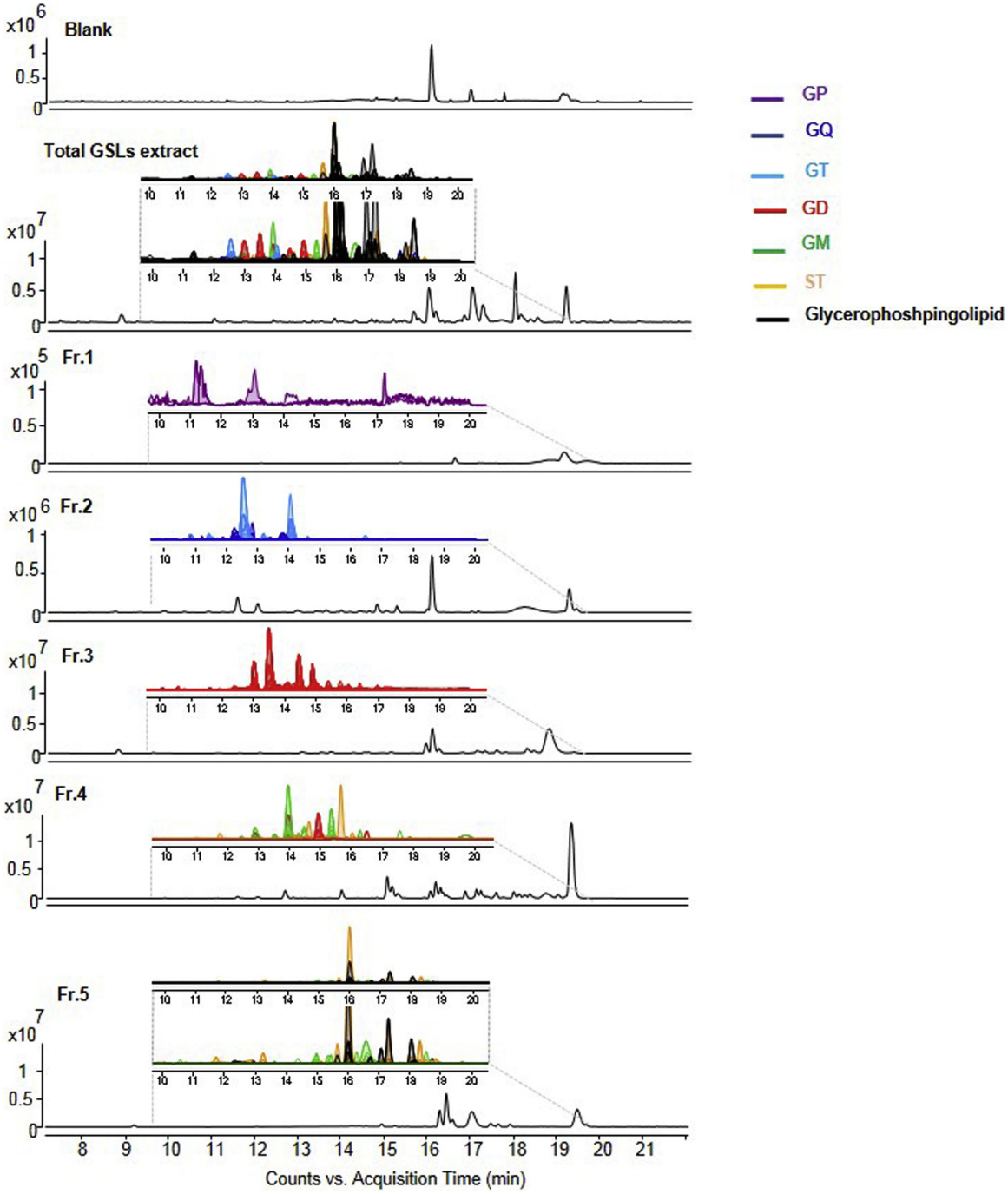

Fig. 1. Chromatograms of blank, total acidic GSLs extract of rat brain tissue and each fraction (Fr. 1–5) obtained after pre-fractionation by C_{18} cartridge. Both base peak chromatogram (BPC) and extracted ion chromatogram (EIC) of identified GSLs obtained by UHPLC-Q-TOF-MS were given.

acetylation, a mass shift of 42 Da was often observed. This can be exemplified by the comparison of GT1b (d18:1/20:0) (Cpd.**208**) which presents $[M+2H]^{2+}$ ion at *m/z* 1079.0579 and OAc-GT1b (d18:1/20:0) (Cpd.**232**) which shows $[M+2H]^{2+}$ ion at *m/z* 1100.0635. Furthermore, the fragments at *m/z* 316.1029 ($[OAc + NeuAc\text{-}H_2O + H]^+$), *m/z* 334.1125 ($[OAc + NeuAc + H]^+$), *m/z* 625.2066 ($[OAc + 2*NeuAc + H]^+$), *m/z* 787.2663 ($[OAc + 2*NeuAc + Hex + H]^+$), and *m/z* 990.3497 ($[OAc + 2*NeuAc + Hex + HexNAc + H]^+$) were only observed in Cpd.**232,** showing that Cpd.**232** possessed one O-acetyl group on one of the tandem sialic acids (Fig. 3C). Fragments at *m/z* 496.1641 ($[OAc + NeuAc + Hex + H]^+$) and *m/z* 699.2475 ($[OAc + NeuAc + Hex + HexNAc + H]^+$) further indicated that the O-acetyl group was attached to the sialic acid adjacent to the galactose residue.

For fucosylation, a mass shift of 146 Da was generally observed. For example, Cpd.**12** presented $[M+2H]^{2+}$ ion at *m/z* 808.9835, while Cpd.**117** presented $[M+2H]^{2+}$ ion at *m/z* 882.0113, indicating that Cpd.**117** was a fucosylated counterpart of Cpd.**12** (Fig. 3D). The fragment at *m/z* 147.0652 ($[Fuc+H]^+$) and *m/z* 512.1963 ($[Fuc+Hex+HexNAc+H]^+$) was only observed in Cpd.**117**, which indicated a linkage of a fucosyl group to galactose residue in Cpd.**117**. Based on above evidence, Cpd.**117** was assigned as Fuc-GM1 (d18:1/23:0).

In addition, a mass shift of 203 Da implicated an attachment of GalNAc. This can be exemplified by the comparison between Cpd.**133,** which owns $[M+2H]^{2+}$ ion at *m/z* 933.5101, and Cpd.**190,** which possesses $[M+2H]^{2+}$ ion at *m/z* 1035.0499. As shown in Fig. 3E,

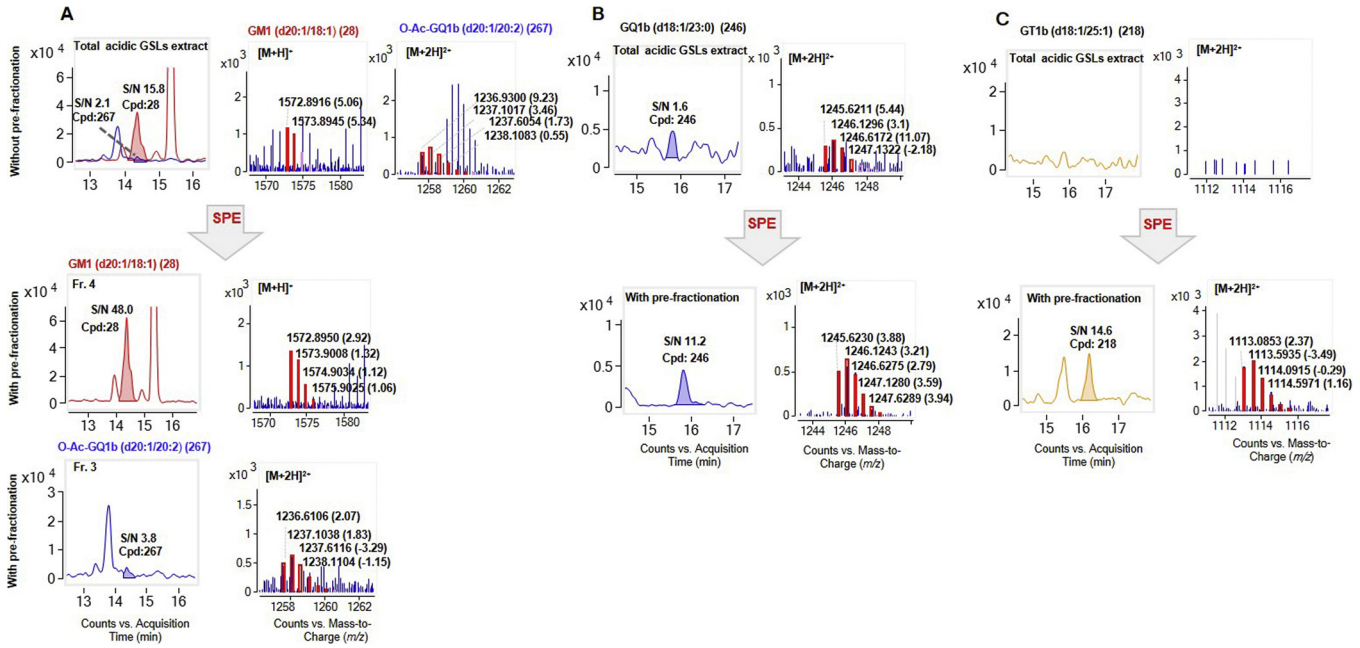

Fig. 2. Comparison of extracted ion chromatograms (EICs) and MS spectra of co-eluted GM1 (d20:1/18:1) (Cpd.**28**) and OAc-GQ1b (d20:1/20:2) (Cpd.**267**) (**A**), GQ1b (d18:1/23:0) (Cpd.**246**) (**B**), and GT1b (d18:1/25:1) (Cpd.**218**) (**C**) with and without C_{18} cartridge pre-fractionation.

fragments at *m/z* 569.2170 ($[HexNAc+Hex+HexNAc+H]^+$) and *m/z* 860.3146 ($[HexNAc+Hex+HexNAc+NeuAc+H]^+$) only presented in Cpd.**190**, suggesting that Cpd.**190** possessed an additional N-acetylgalactosamine group adjacent to galactose residue. Thus, Cpd.**190** was characterized as GalNAc-GD1a (d18:1/20:0).

3.2.1.3. Structural elucidation of STs. Structure elucidation of STs was accomplished in a similar manner as that of GAs. For instance, Cpd.**284** was tentatively assigned as a ST with the formula of $C_{54}H_{101}NO_{16}S$ based on its $[M+H]^+$ ion at *m/z* 1052.6918. MS/MS analysis of $[M+H]^+$ ion at *m/z* 1052.6918 provided structural information of its glycan chain and ceramide moiety. First, an 80 gap from *m/z* 1052.6918 to *m/z* 972.7318 was observed as evidence of the existence of the sulfate group. Second, two 162 gaps from *m/z* 972.7318 to *m/z* 810.6701, and then to *m/z* 648.6279 indicated the sequential loss of two hexosyl groups. Third, the ion at *m/z* 648.6279 ($[M\text{-glycan chain}+H]^+$), together with the ions at *m/z* 630.6175 ($[M\text{-glycan chain-}H_2O+H]^+$), *m/z* 612.6098 ($[M\text{-glycan chain-2*}H_2O+H]^+$), and *m/z* 600.6087 ($[M\text{-glycan chain-}H_2O-HCOH+H]^+$) suggested an dihydroxylated Cer (d42:2) as the ceramide moiety of Cpd.**284**. Furthermore, ions at *m/z* 282.2755 ($[d18:1\text{-}H_2O+H]^+$), *m/z* 264.2685 ($[d18:1\text{-}2*H_2O+H]^+$), and *m/z* 252.2531 ($[d18:1\text{-}H_2O-HCOH+H]^+$) suggested a d18:1 sphingoid backbone of Cpd.**284**, while ion at *m/z* 366.3524 suggested the presence of a C_{24} fatty acid chain with one double bond. On the basis of the above information, Cpd.**284** was identified as $sulfoHex_2$ (d18:1/24:1) (Fig. 3F).

3.2.2. Differentiation of isobaric and isomeric acidic GSLs

High-resolution MS and MS/MS interpretation also facilitated well differentiation of isobaric acidic GSLs. An example was illustrated in Fig. 4A, where the compound owing $[M+2H]^{2+}$ ion at *m/z* 1245.6115 was identified as OAc-GQ1b (d20:1/18:0) (Cpd.**265**) based on its measured mass value ($C_{110}H_{188}N_6O_{56}$, theoretical mass 2489.2048), while the compound owing $[M+2H]^{2+}$ ion at *m/z* 1245.6271 was identified as GQ1b (d18:1/23:0) (Cpd.**246**) based on its measured mass value ($C_{111}H_{192}N_6O_{55}$, theoretical mass 2489.2412). By using a likewise strategy, 19 pairs of isobaric species, including 10 pairs of GA and 9 pairs of ST, were unambiguously distinguished (Supporting information Table. S1).

Of note, high-resolution MS and MS/MS data solely were inadequate in differentiating isomeric species. Sufficient chromatographic separation of isomeric species was also essentially important. Optimized chromatographic separation, efficient pre-fractionation, altogether with the high-resolution MS and MS/MS facilitated the differentiation of two types of isomeric acidic GSLs in our study. Differentiation of isomeric acidic GSLs that only differs in glycan chains was exemplified in Fig. 4B, where $[M+2H]^{2+}$ ion at *m/z* 919.4933 yielded two peaks at 12.9 min and 13.3 min. The peak at 12.9 min was identified as GD1a (d18:1/18:0) (Cpd.**131**) based on the diagnostic fragment at *m/z* 657.2403 ($[NeuAc+Hex+HexNAc+H]^+$), while the peak at 13.3 min was identified as GD1b (d18:1/18:0) (Cpd.**148**) based on the diagnostic fragment at *m/z* 583.1951 ($[2*NeuAc+H]^+$). Similarly, 21 pairs of isomeric GAs that only differ in glycan chains were distinguished (Supporting information Table. S1). Another type of isomeric acidic GSLs that only differs in ceramide moiety was exemplified in Fig. 4C, where $[M+2H]^{2+}$ ion at *m/z* 1224.6044 yielded two peaks at 13.3 min and 13.7 min. The peak at 13.3 min was identified as GQ1b (d20:1/18:0) (Cpd.**254**) based on the diagnostic fragment at *m/z* 292.3010 ($[d20:1\text{-}H_2O+H]^+$), while the peak at 13.7 min was identified as GQ1b (d18:1/20:0) (Cpd.**244**) based on the diagnostic fragment at *m/z*264.2681 ($[d18:1\text{-}H_2O+H]^+$). In this way, 29 pairs of isomeric GAs and 10 pairs of isomeric STs that only differentiate in ceramide moiety were distinguished (Supporting information Table. S1).

3.2.3. Reversed-phase liquid chromatographic (RP-LC) retention (RT) rule of acidic GSLs

On the basis of the chromatographic separation, a linear correlation between carbon number vs RT with good fitting ($R^2 > 0.99$) was observed for GM1, GD1a, GT1b, GQ1b, and ST types as shown in Fig. 5A, and for GM1, GM2, GM3, and GM4 types as shown in Fig. 5B. Clearly, RT of acidic GSLs increase with carbon number for all types of acidic GSLs. Moreover, when the carbon number was fixed, RT of acidic GSLs decreased along with the number of sialic acids (ST > GM1 > GD1a > GT1b > GQ1b) or more sugar residues (GM4 > GM3 > GM2 > GM1). Such RP-LC retention rule can provide supporting evidence for the characterization of acidic GSLs, such as GM2 (d18:1/17:0) (Cpd.**38**), GM4 (d18:1/19:0) (Cpd.**93**), and GM4 (d18:1/21:0)

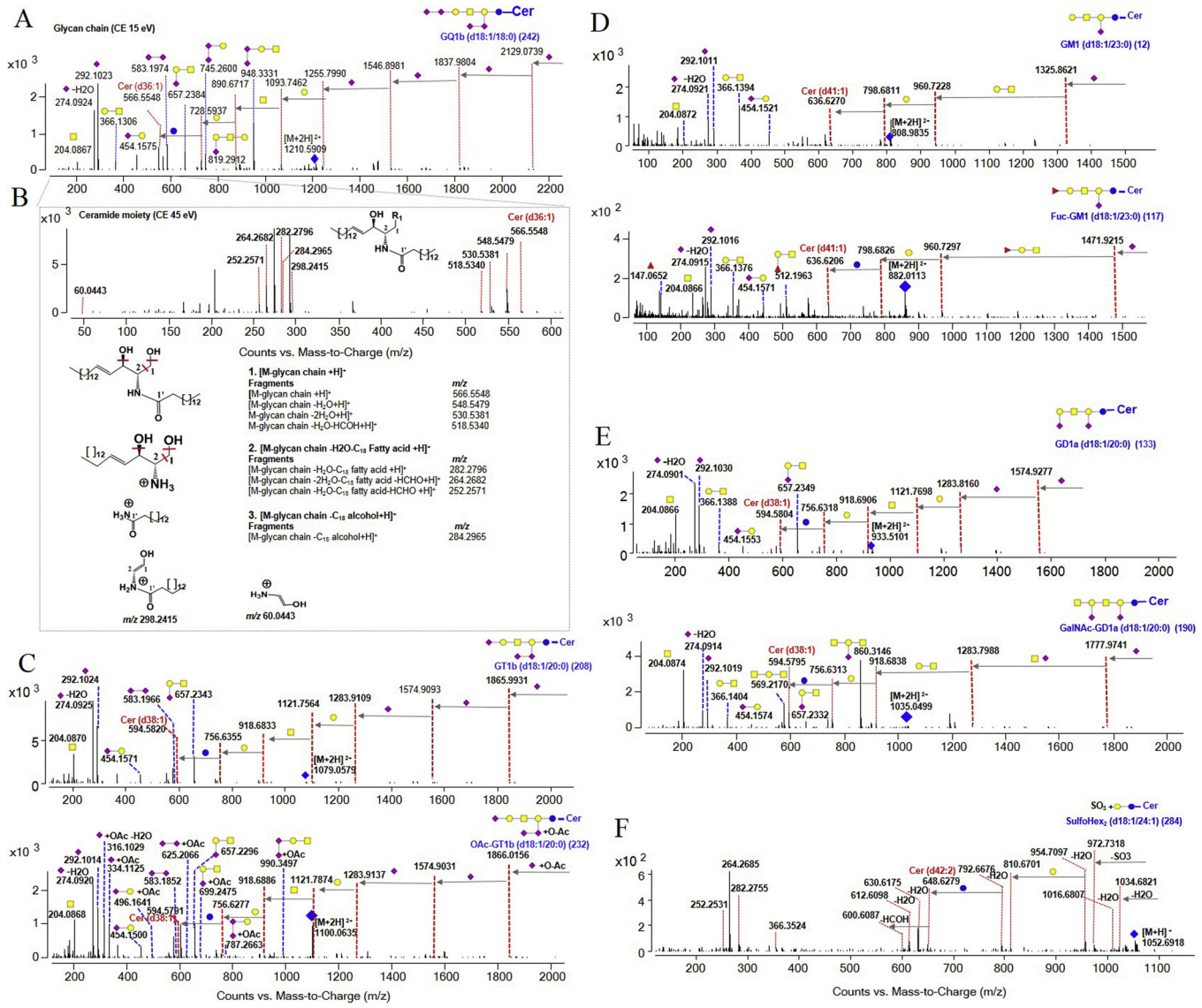

Fig. 3. MS/MS spectra of glycan chain moiety (**A**) and ceramide moiety (**B**) of GQ1b (d18:1/18:0) (Cpd.**242**).Comparison of MS/MS spectra of GT1b (d18:1/20:0) (Cpd.**208**) and OAc-GT1b (d18:1/20:0) (Cpd.**232**) (**C**), GM1 (d18:1/23:0) (Cpd.**12**) and Fuc-GM1 (d18:1/23:0) (Cpd.**117**) (**D**), GD1a (d18:1/20:0) (Cpd.**133**) and GalNAc-GD1a (d18:1/20:0) (Cpd.**190**) (E). MS/MS spectra of sulfoHex$_2$ (d18:1/24:1) (Cpd.**284**) (**F**).

(Cpd.**95**).

In addition, a good linear correlation ($R^2 > 0.99$) between carbon number vs RT was observed for GM1 and Fuc-GM1 types, GQ1b and OAc-GQ1b types, as well as GD1a and GalNAc-GD1a types as illustrated in Fig. 5C, Fig. 5D, and Fig. 5E, respectively. For instance, fucosylation and attachment of GalNAc led to a decrease in RT, while O-acetylation caused an increase in RT. By using this RP-LC retention rule, Fuc-GM1 (d18:1/24:0) (Cpd.**118**) and GalNAc-GD1a (d18:1/24:0) (Cpd.**193**) were identified.

Furthermore, a good linear correlation ($R^2 > 0.99$) between unsaturation degree vs RT was noticed for GM1, GM2, GM3, GD1a, GD1b, GT1b, and GQ1b types as shown in Fig. 5F. This displayed that the unsaturation degree of acidic GSLs was inversely correlated to RT. GD1b (d18:1/24:0) (Cpd.**154**) and GD1b (d18:1/25:0) (Cpd.**155**) were confirmed according to this RP-LC retention rule.

In summary, RT of acidic GSLs increased along with carbon number, and decreased along with the number of sialic acids, sugar residues, and unsaturation degree. Moreover, O-acetylation caused an increase in RT, while fucosylation and attachment of GalNAc led to a decrease in RT.

3.2.4. Confirmation of identified acidic GSLs by employing commercial standards

Nine GAs and 1 ST commercial standards were further employed to confirm the identification of acidic GSLs. As shown in Fig. 6A, 9 GAs (Cpd.**7**, **39**, **61**, **112**, **131**, **148**, **162**, **206,** and **242**) and 1 ST (Cpd.**298**) identified from rat brain tissues exhibited the same RT with corresponding acidic GSLs standards. Furthermore, as exemplified in Fig. 6B-C, acidic GSLs identified from rat brain tissues were confirmed by corresponding acidic GSLs standards via a comparison of their high-resolution MS and MS/MS spectra. Notably, commercial standards were adopted to support the identification of acidic GSLs in our study.

3.3. Chemical characteristics of acidic GSLs identified from rat brain tissues

Through the rigorous identification of acidic GSLs, a total of 340 acidic GSLs (from 281 compositions) were found in rat brain tissues, including 277 GAs (from 230 compositions) and 63 STs (from 51 compositions). Among which, 57 novel GAs and 14 novel STs were identified. The number of compounds identified from different types of acidic GSLs and from different types of modification were demonstrated

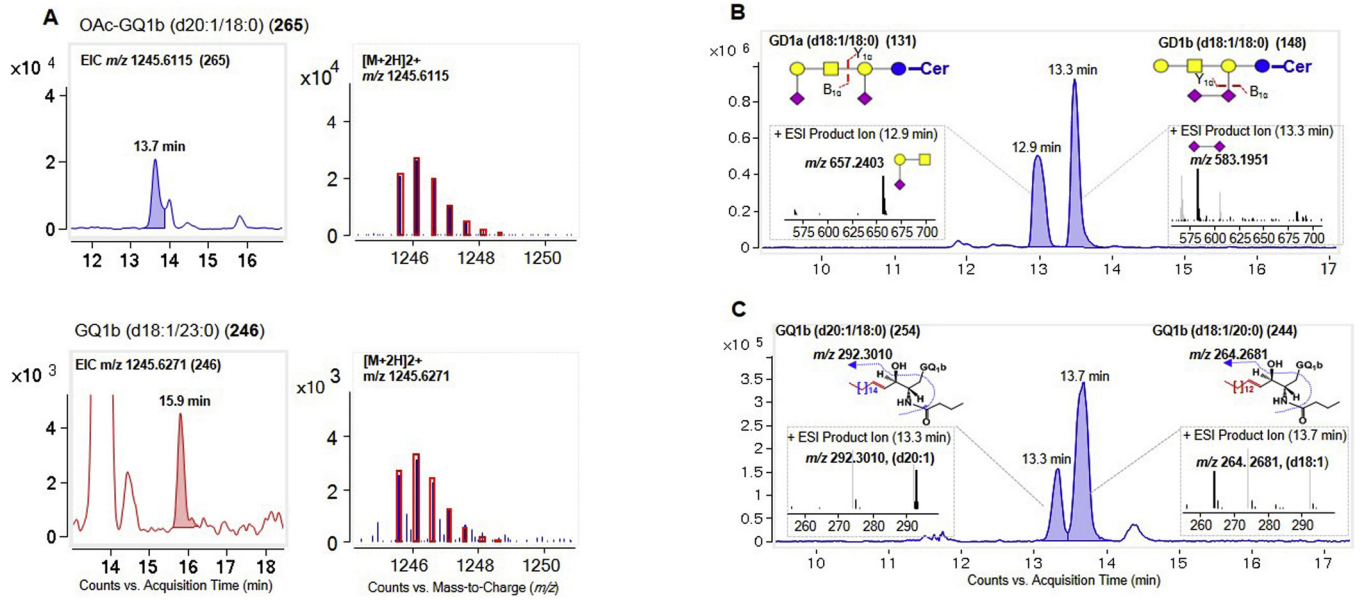

Fig. 4. Differentiation of isobaric acidic GSLs, OAc-GQ1b (d20:1/18:0) (Cpd.**265**) and GQ1b (d18:1/23:0) (Cpd.**246**), by high resolution mass spectrometry (**A**). Differentiation of isomeric acidic GSLs which only differentiate in glycan chain moiety, GD1a (d18:1/18:0) (Cpd.**131**) and GD1b (d18:1/18:0) (Cpd.**148**) (**B**), and isomeric acidic GSLs which only differentiate in ceramide moiety, GQ1b (d20:1/18:0) (Cpd.**254**) and GQ1b (d18:1/20:0) (Cpd.**244**) (**C**), by sufficient chromatographic separation and diagnostic MS/MS fragments.

in Fig. 7A and 7B, respectively. Moreover, as shown in Fig. 7C, O-acetylation was dominant in GQ type, while fucosylation was dominant in GM type, and attachment of GalNAc was dominant in GD type. Meanwhile, our results showed that d18:1 and d20:1 are the predominant sphingoid backbones in rat brain tissues, while the fatty acyl chains are typically in d16:0, d18:0, d20:0 and d22:0 (Supporting information Table. S2-5).

Notably, the newly characterized acidic GSLs significantly enlarged our understanding of the diversification of natural acidic GSLs. Novel GAs in rat brain tissues can be reflected in (1) O-acetylation (OAc) modified GP type GAs (Cpd.**276**, **277**); (2) OAc modified GQ type GAs with low carbon number (< 36) (Cpd.**258**) or high unsaturation degree (> 1) (Cpd.**262**, **263**, **264**, **267**, **268**); (3) OAc modified GT, GD, or GM type with less sugar residues (Cpd.**107**, **108**, **181**, **182**, **183**, **236**); (4) Fuc modified GQ type GAs (Cpd.**269**, **270**, **271**); (5) attachment of GalNAc modified GD1b type GA (Cpd.**200**); (6) GQ type GAs with phytosphingoid backbone (Cpd.**257**) or high carbon number (> 40) (Cpd.**246**); (7) GT type GA with high unsaturation degree (> 2) (Cpd.**220**, **228**); (8) GM type GA with high carbon number (> 44) (Cpd.**14**) (Fig. 8A). In addition, novel STs in rat brain tissues can be reflected in (1) dihexosyl STs with high carbon number (> 42) (Cpd.**283**, **285**, **288**, **289**); (2) STs with phytosphingoid backbone and low carbon number (< 38) (Cpd.**325**, **331**, **339**) (Fig. 8B).

4. Discussion and conclusion

The acidic GSL samples extracted from biological samples generally contain substantial non-targeted components. The non-targeted components and high abundance acidic GSLs (e.g. GM and GD species) may potentially influence the detection of low-abundance acidic GSLs (e.g. GQ, GP and their modified GSLs) in MS due to ion-suppression and isobaric/isomeric interferences (Chiu et al., 2010; Masson et al., 2015; Mi et al., 2018, 2016b; Huang et al., 2018). Although previous studies have employed C_{18}, C_8, HLB, and SCX SPE or DEAE-sephadex cartridge to remove salt, protein, and non-lipid contaminants to enrich acidic GSLs (Zhang et al., 2012; Bai et al., 2013; Masson et al., 2015), a method that is capable of enriching different types of acidic GSLs and removing of high abundance glycerophospholipids has not been developed because of the high similarity in the physiochemical properties of the complex acidic GSLs.

In the current study, we developed a fast and simple pre-fractionation method that can enrich different types of acidic GSLs and remove glycerophospholipids by using a C_{18} cartridge. Upon pre-fractionation, the detection of a considerable number of acidic GSLs were enhanced significantly due to reduced ion suppression arising from co-eluted species and exogenous interferences. Of note, the detection of GMs achieved the greatest improvement after pre-fractionation, and such an improvement led to the identification of a great number of novel GMs (44% of overall novel GAs). GM1 was reported to be highly expressed in the brain, and is known to be involved in several neuronal functions (Posse de Chaves and Sipione, 2010; Ledeen and Wu, 2015). Additionally, it is related to the production of amyloid beta (Aβ) fibrils in Alzheimer's disease (Yamazaki et al., 2007; Schauer et al., 2011; Ariga et al., 2011). Comprehensive characterization of GM species of brain tissues may provide more chemical information for exploring the roles of GMs in the pathogenesis and progression of neurodegenerative diseases.

In our study, a total of 340 acidic GSLs (from 281 compositions) were characterized in rat brain tissues. This number was almost double of that previous reported (Hajek et al., 2017). In particular, a significant improvement in the characterization of modified GAs was achieved, especially OAc-modified species in rat brain tissues. Of note, we identified a type of uncommon OAc modification which occurs on inner sialic acid instead of terminal sialic acid. (Sjoberg et al., 1992; Romero-Ramírez et al., 2012; Baumann et al., 2015; Fleurence et al., 2017). OAc modification of GA-linked sialic acid was reported to create discrete molecular patterns that may influence cell interactions in neural development (Blum and Barnstable, 1987). The OAc modification was also suggested to be involved in childhood acute lymphoblastic leukemia and immune defense (Schauer et al., 2011; Mandal et al., 2012; Baumann et al., 2015; Mandal et al., 2015). Our discovery of the uncommon OAc modification provided novel structural information for the understanding of acetylated GAs.

In addition to OAc GAs, a number of novel Fuc GAs and GalNAc GAs were also identified in rat brain tissue. Fuc-GM1 was reported to be involved in promoting Aβ accumulation in PC12 cells (Yanagisawa et al., 2006), as well as PC12 cell neuritogenesis (Yamazaki et al., 2007). Similar to the fucosyl group, GalNAc group was found to be

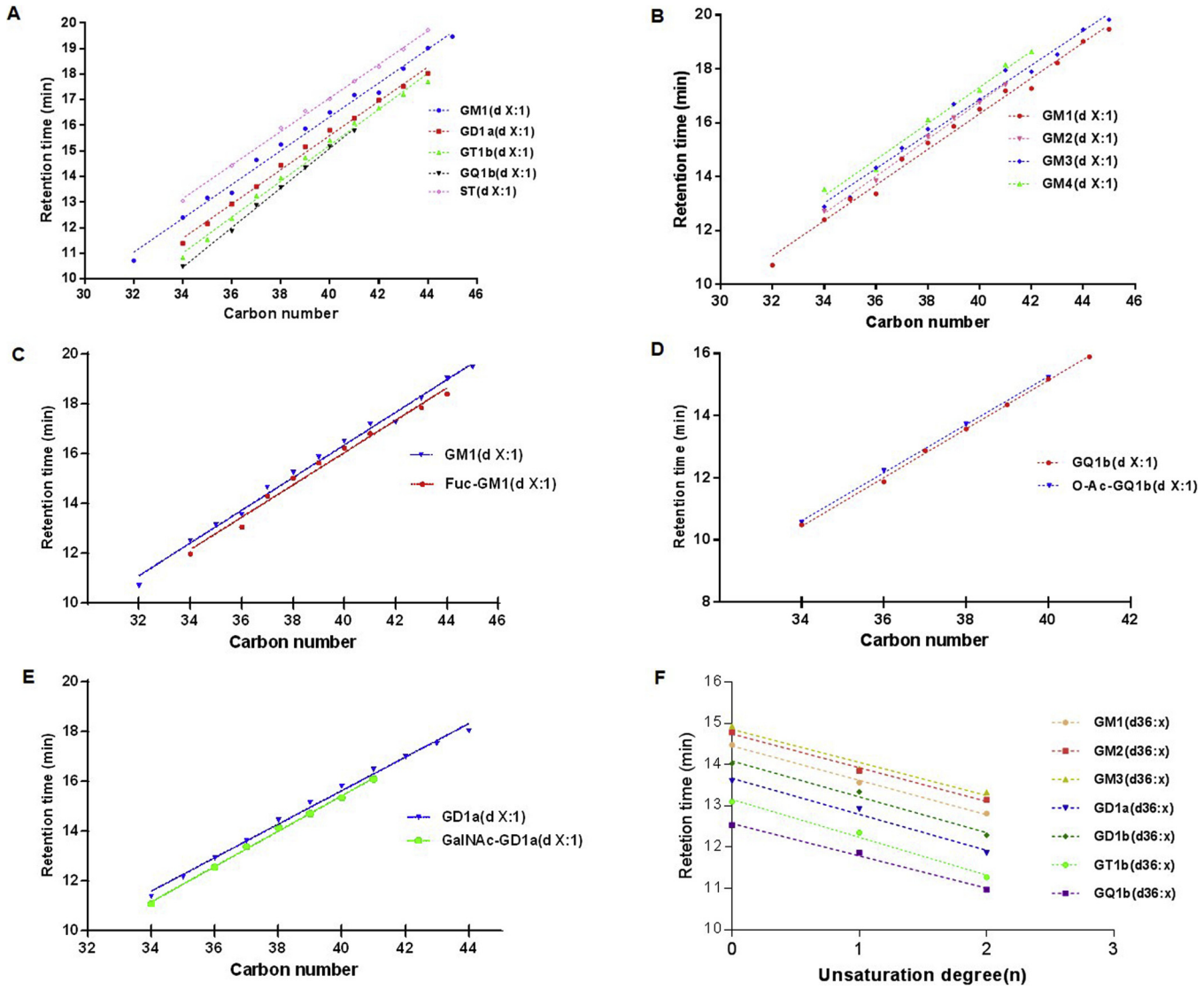

Fig. 5. Linear regression model constructed by plotting carbon number (**A-E**), and unsaturation degree (**F**) of different types of acidic GSLs vs retention time.

attached on galactose residue. Anti-GalNAc-GD1a antibodies were reported as diagnostic markers for Guillain-Barre'syndrome (GBS) (Kusunoki et al., 1994, Kaida et al., 2003; Tatsumoto et al., 2006), while minor GalNAc-GD1a was helpful for therapy of chronic motor axonal neuropathy (Kaji et al., 2000; Tatsumoto et al., 2006). The identification of novel Fuc GAs and GalNAc GAs enlarged our understanding of the structural diversity of natural acidic GSLs, and aids in developing a better exploration of the biological function of acidic GSLs.

Prior studies have shown that alterations in sphingoid backbones are correlated to development of neurodegenerations as well as the effectiveness of signal transduction at the cell surface (Sonnino and Chigorno, 2000; Caughlin et al., 2015). More importantly, the d20:1 species are implicated as a metabolic marker of aging (Palestini et al., 1990) (Weishaupt et al., 2015), and long chain saturated fatty acids may influence the fluidity and structural rigidity of the membrane (Schnaar et al., 2014; Palmano et al., 2015). These reports collectively demonstrated the important structure-function relationship of acidic GSLs. Hence, the high-resolution MS/MS data acquired in our study allow for the elucidation of both sphingoid backbone and fatty acyl chain, which would be helpful for further investigation of the physiological and pathological role of GAs in CNS.

In conclusion, we developed an improved approach for the comprehensive profiling of acidic GSLs in biological samples. This approach integrated a fast and effective pre-fractionation step for the enrichment of different types of acidic GSLs and the removal of non-targeted components. This is the first report of this effective fractionation method of acidic GSLs. This pre-fractionation step was demonstrated to be crucial for the accurate analysis of acidic GSLs, especially those low-abundance species. Furthermore, our study represents the most comprehensive approach for the identification of acidic GSLs as evidenced by the discovery of a considerable number of novel GAs and STs in rat brain tissues. This improved approach would provide a powerful tool for the understanding of the biological function of acidic GSLs in the CNS.

Acknowledgments

This research was funded by the Science and Technology Development Fund, Macau SAR (File no. 023/2016/AFJ to W.J.R.) and National Natural Science Foundation of China (Project 81661168012); this work was also sponsored by Open Project of State Key Laboratory of Respiratory Disease (No. SKLRD2016OP007).

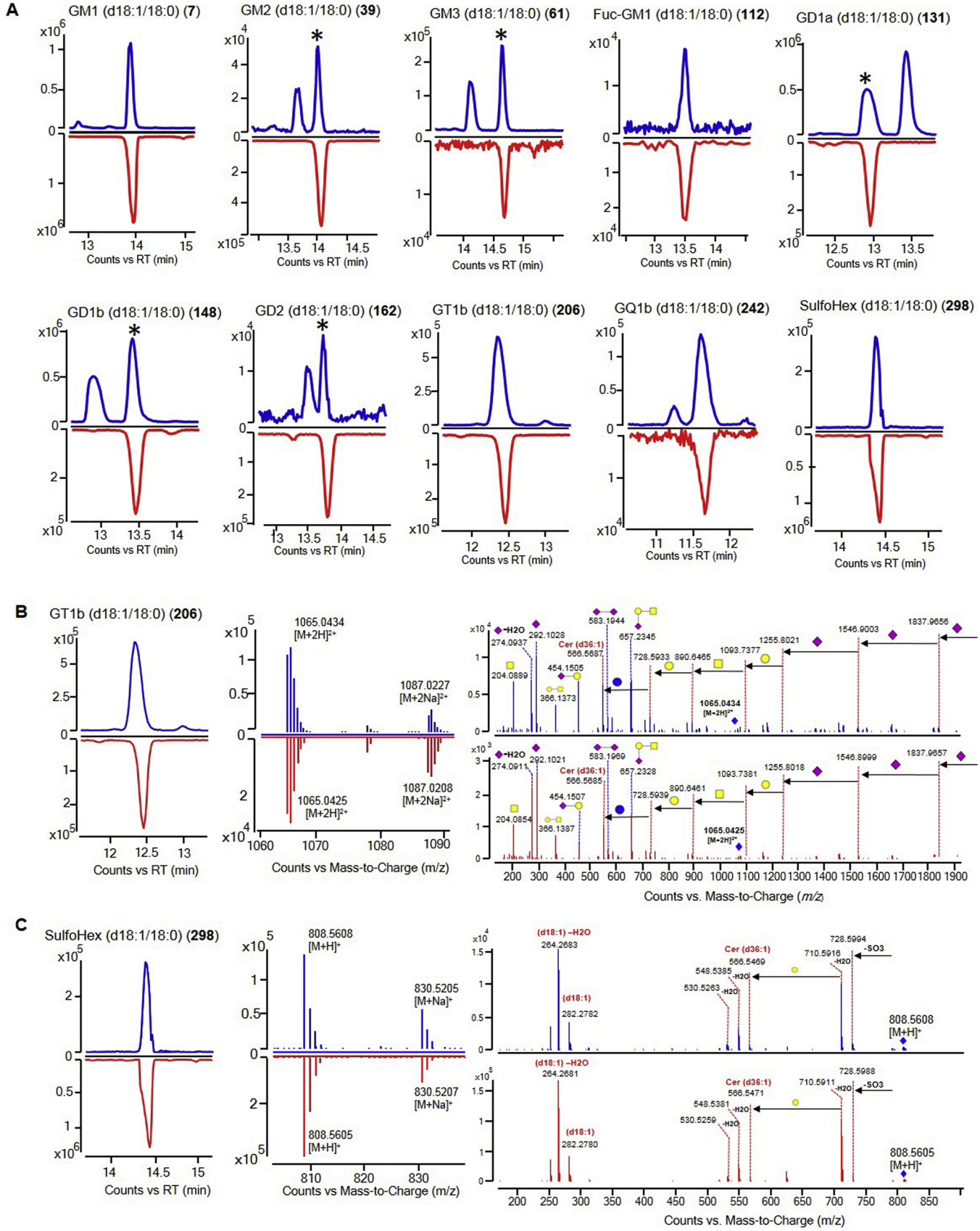

Fig. 6. Comparison of the retention time of 9 GAs and 1 ST in rat brain tissue with corresponding acidic GSL standards (**A**); the identified acidic GSLs were confirmed by corresponding acidic GSLs standards via a comparison of MS and MS/MS spectra (**B-C**).

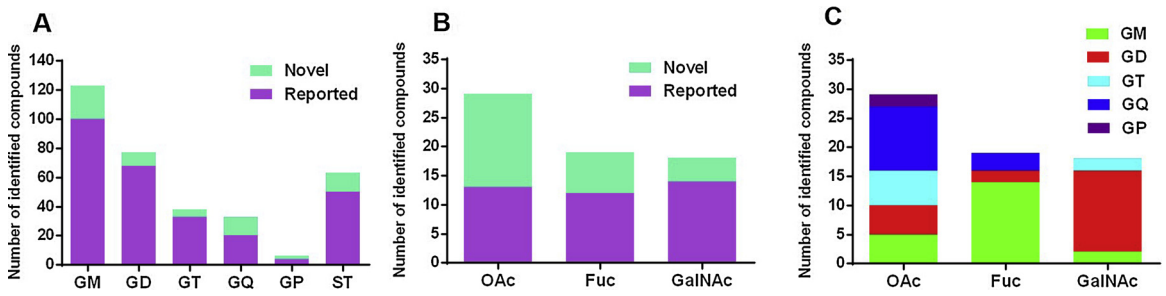

Fig. 7. The number of compounds identified from different types of acidic GSLs (GM, GD, GT, GQ, GP, and ST) (**A**); the number of compounds identified from different types of modification (OAc, Fuc, and GalNAc) (**B**). The distribution of different types of acidic GSLs within different types of modification (**C**).

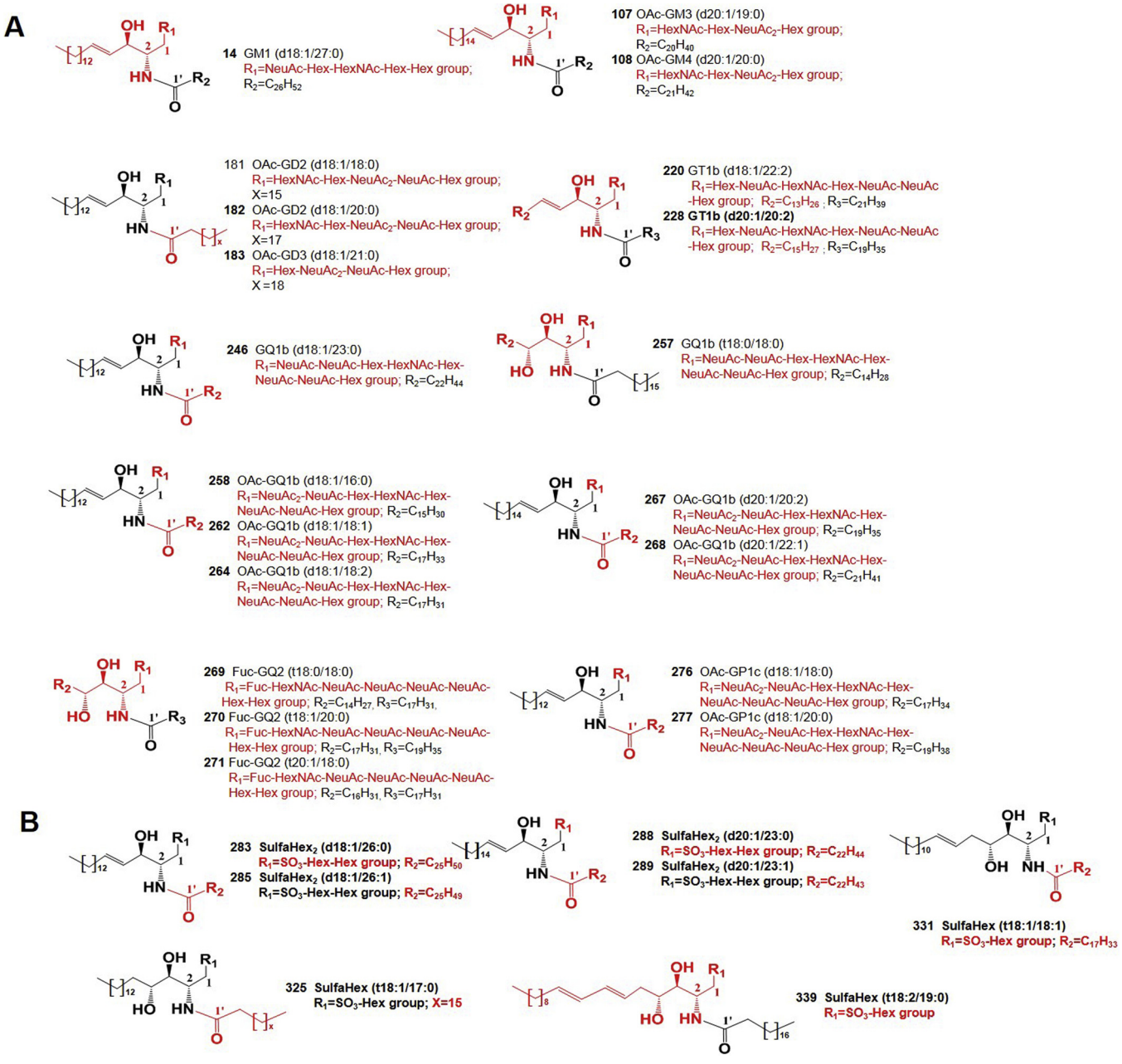

Fig. 8. Structures of representative novel GA analogues (**A**); structures of representative novel ST analogues (**B**).

Appendix A. Supplementary data

Supplementary material related to this article can be found, in the online version, at doi:https://doi.org/10.1016/j.chemphyslip.2019.104813.

References

Alpaugh, M., Galleguillos, D., Forero, J., Morales, L.C., Lackey, S.W., Kar, P., Di Pardo, A., Holt, A., Kerr, B.J., Todd, K.G., Baker, G.B., Fouad, K., Sipione, S., 2017. Disease-modifying effects of ganglioside gm1 in huntington's disease models. EMBO Mol. Med. 9, 1537–1557.

Ariga, T., Wakade, C., Yu, R.K., 2011. The pathological roles of ganglioside metabolism in Alzheimer's disease: effects of gangliosides on neurogenesis. Int. J. Alzheimers Dis. 2011, 193618.

Bai, N., Cui, X.Y., Wang, J., Sun, C.G., Mei, H.K., Liang, B.B., Cai, Y., Song, X.J., Gu, J.K., Wang, R., 2013. Determination of thalidomide concentration in human plasma by liquid chromatography-tandem mass spectrometry. Exp. Ther. Med. 5, 626–630.

Baumann, A.-M.T., Bakkers, M.J., Buettner, F.F., Hartmann, M., Grove, M., Langereis, M.A., De Groot, R.J., Mühlenhoff, M., 2015. 9-o-acetylation of sialic acids is catalysed by casd1 via a covalent acetyl-enzyme intermediate. Nat. Commun. 6, 7673.

Blum, A.S., Barnstable, C.J., 1987. O-acetylation of a cell-surface carbohydrate creates discrete molecular patterns during neural development. Proc. Natl. Acad. Sci. U. S. A. 84, 8716–8720.

Caughlin, S., Hepburn, J.D., Park, D.H., Jurcic, K., Yeung, K.K.-C., Cechetto, D.F., Whitehead, S.N., 2015. Increased expression of simple ganglioside species gm2 and gm3 detected by maldi imaging mass spectrometry in a combined rat model of aβ toxicity and stroke. PLoS One 10, e0130364.

Chiu, M.L., Lawi, W., Snyder, S.T., Wong, P.K., Liao, J.C., Gau, V., 2010. Matrix effects-a challenge toward automation of molecular analysis. Jala 15, 233–242.

Eckhardt, M., 2008. The role and metabolism of sulfatide in the nervous system. Mol. Neurobiol. 37, 93–103.

Fleurence, J., Fougeray, S., Bahri, M., Cochonneau, D., Clemenceau, B., Paris, F., Heczey, A., Birkle, S., 2017. Targeting o-acetyl-gd2 ganglioside for cancer immunotherapy. J. Immunol. Res. 2017, 5604891.

Folch, J., Lees, M., Sloane Stanley, G.H., 1957. A simple method for the isolation and purification of total lipides from animal tissues. J. Biol. Chem. 226, 497–509.

Hajek, R., Jirasko, R., Lisa, M., Cifkova, E., Holcapek, M., 2017. Hydrophilic interaction liquid chromatography-mass spectrometry characterization of gangliosides in biological samples. Anal. Chem. 89, 12425–12432.

Han, X.L., Fagan, A.M., Cheng, H., Morris, J.C., Xiong, C.J., Holtzman, D.M., 2003. Cerebrospinal fluid sulfatide is decreased in subjects with incipient dementia. Ann. Neurol. 54, 115–119.

Hu, T., Jia, Z.X., Zhang, J.L., 2017. Strategy for comprehensive profiling and identification of acidic glycosphingolipids using ultra-high-performance liquid chromatography coupled with quadrupole time-of-flight mass spectrometry. Anal. Chem. 89, 7808–7816.

Huang, H., Tong, T.T., Yau, L.F., Chen, C.Y., Mi, J.N., Wang, J.R., Jiang, Z.H., 2016. Lc-ms based sphingolipidomic study on a2780 human ovarian cancer cell line and its taxol-resistant strain. Sci. Rep. 6.

Huang, H., Tong, T.T., Yau, L.F., Chen, C.Y., Mi, J.N., Wang, J.R., Jiang, Z.H., 2018. Lc-ms based sphingolipidomic study on a549 human lung adenocarcinoma cell line and its taxol-resistant strain. BMC Cancer 18, 799.

Kaida, K., Kusunoki, S., Kamakura, K., Motoyoshi, K., Kanazawa, I., 2003. Galnac-gd1a in human peripheral nerve: target sites of anti-ganglioside antibody. Neurology 61, 465–470.

Kaji, R., Kusunoki, S., Mizutani, K., Oka, N., Kojima, Y., Kohara, N., Kimura, J., 2000. Chronic motor axonal neuropathy associated with antibodies monospecific for n-acetylgalactosaminyl gd1a. Muscle Nerve 23, 702–706.

Kolter, T., 2012. Ganglioside biochemistry. ISRN Biochem. 2012, 506160.

Kolter, T., Proia, R.L., Sandhoff, K., 2002. Combinatorial ganglioside biosynthesis. J. Biol. Chem. 277 25859-62.

Kusunoki, S., Chiba, A., Kon, K., Ando, S., Arisawa, K., Tate, A., Kanazawa, I., 1994. N-acetylgalactosaminyl gd1a is a target molecule for serum antibody in guillain-barré syndrome. Ann. Neurol. 35, 570–576.

Ledeen, R.W., Wu, G., 2015. The multi-tasked life of gm1 ganglioside, a true factotum of nature. Trends Biochem. Sci. 40, 407–418.

Li, P., Wang, S.J., Zhang, R.L., Pei, J., Chen, L.L., Cao, Y.B., Zhang, H.L., Yang, G.F., 2018. Identification of csf biomarkers by proteomics in guillain-barre syndrome. Exp. Ther. Med. 15, 5177–5182.

Li, Y.T., 2012. On the structural elucidation of galnac-gd1a. Neurochem. Res. 37, 1150–1153.

Mandal, C., Mandal, C., Chandra, S., Schauer, R., Mandal, C., 2012. Regulation of o-acetylation of sialic acids by sialate-o-acetyltransferase and sialate-o-acetylesterase activities in childhood acute lymphoblastic leukemia. Glycobiology 22, 70–83.

Mandal, C., Schwartz-Albiez, R., Vlasak, R., 2015. Functions and biosynthesis of o-acetylated sialic acids. Top. Curr. Chem. 366, 1–30.

Masson, E.A., Sibille, E., Martine, L., Chaux-Picquet, F., Bretillon, L., Berdeaux, O., 2015. Apprehending ganglioside diversity: a comprehensive methodological approach. J. Lipid Res. 56, 1821–1835.

Mi, J.N., Han, Y.W., Xu, Y.Q., Kou, J.P., Li, W.J., Wang, J.R., Jiang, Z.H., 2018. Deep profiling of immunosuppressive glycosphingolipids and sphingomyelins in wild cordyceps. J. Agric. Food Chem. 66, 8991–8998.

Mi, J.N., Han, Y.W., Xu, Y.Q., Kou, J.P., Wang, J.R., Jiang, Z.H., 2016a. New immunosuppressive sphingoid base and ceramide analogues in wild cordyceps. Sci. Rep. 6.

Mi, J.N., Wang, J.R., Jiang, Z.H., 2016b. Quantitative profiling of sphingolipids in wild cordyceps and its mycelia by using uhplc-ms. Sci. Rep. 6.

Mohammadi, A.S., Phan, N.T.N., Fletcher, J.S., Ewing, A.G., 2016. Intact lipid imaging of mouse brain samples: maldi, nanoparticle-laser desorption ionization, and 40 kev argon cluster secondary ion mass spectrometry. Anal. Bioanal. Chem. 408, 6857–6868.

Palestini, P., Masserini, M., Sonnino, S., Giuliani, A., Tettamanti, G., 1990. Changes in the ceramide composition of rat forebrain gangliosides with age. J. Neurochem. 54, 230–235.

Palmano, K., Rowan, A., Guillermo, R., Guan, J., McJarrow, P., 2015. The role of gangliosides in neurodevelopment. Nutrients 7 3891-913.

Posse de Chaves, E., Sipione, S., 2010. Sphingolipids and gangliosides of the nervous system in membrane function and dysfunction. FEBS Lett. 584, 1748–1759.

Rivas-Serna, I.M., Polakowski, R., Shoemaker, G.K., Mazurak, V.C., Clandinin, M.T., 2015. Profiling gangliosides from milk products and other biological membranes using lc/ms. J. Food Compos. Anal. 44, 45–55.

Romero-Ramírez, L., García-Álvarez, I., Campos-Olivas, R., Gilbert, M., Goneau, M.-F., Fernández-Mayoralas, A., Nieto-Sampedro, M., 2012. Specific synthesis of neurostatin and gangliosides o-acetylated in the outer sialic acids using a sialate transferase. PLoS One 7, e49983.

Sarbu, M., Robu, A.C., Ghiulai, R.M., Vukelic, Z., Clemmer, D.E., Zamfir, A.D., 2016. Electrospray ionization ion mobility mass spectrometry of human brain gangliosides. Anal. Chem. 88, 5166–5178.

Schauer, R., Srinivasan, G.V., Wipfler, D., Kniep, B., Schwartz-Albiez, R., 2011. O-acetylated Sialic Acids and Their Role in Immune Defense. The Molecular Immunology of Complex carbohydrates-*3*. Springer.

Schnaar, R.L., Gerardy-Schahn, R., Hildebrandt, H., 2014. Sialic acids in the brain: gangliosides and polysialic acid in nervous system development, stability, disease, and regeneration. Physiol. Rev. 94, 461–518.

Sjoberg, E., Manzi, A., Khoo, K., Dell, A., Varki, A., 1992. Structural and immunological characterization of o-acetylated gd2. Evidence that gd2 is an acceptor for ganglioside o-acetyltransferase in human melanoma cells. J. Biol. Chem. 267, 16200–16211.

Skraskova, K., Claude, E., Jones, E.A., Towers, M., Ellis, S.R., Heeren, R.M., 2016. Enhanced capabilities for imaging gangliosides in murine brain with matrix-assisted laser desorption/ionization and desorption electrospray ionization mass spectrometry coupled to ion mobility separation. Methods 104, 69–78.

Sonnino, S., Chigorno, V., 2000. Ganglioside molecular species containing c18- and c20-sphingosine in mammalian nervous tissues and neuronal cell cultures. Biochim. Biophys. Acta 1469, 63–77.

Sonnino, S., Mauri, L., Chigorno, V., Prinetti, A., 2007. Gangliosides as components of lipid membrane domains. Glycobiology 17, 1R–13R.

Svennerholm, L., 1963. Chromatographic separation of human brain gangliosides. J. Neurochem. 10, 613–623.

Svennerholm, L., Fredman, P., 1980. A procedure for the quantitative isolation of brain gangliosides. Biochim. Biophys. Acta 617, 97–109.

Tatsumoto, M., Koga, M., Gilbert, M., Odaka, M., Hirata, K., Kuwabara, S., Yuki, N., 2006. Spectrum of neurological diseases associated with antibodies to minor gangliosides gm1b and galnac-gd1a. J. Neuroimmunol. 177, 201–208.

Tian, H., Sparvero, L.J., Amoscato, A.A., Bloom, A., Bayir, H., Kagan, V.E., Winograd, N., 2017. Gas cluster ion beam time-of-flight secondary ion mass spectrometry high-resolution imaging of cardiolipin speciation in the brain: identification of molecular losses after traumatic injury. Anal. Chem. 89, 4611–4619.

Tonidandel, L., Seraglia, R., 2007. Matrix effect, signal suppression and enhancement in lc-esi-ms. J. Chromatogr. Library 72, 193.

Vukelic, Z., Zarei, M., Peter-Katalinic, J., Zamfir, A.D., 2006. Analysis of human hippocampus gangliosides by fully-automated chip-based nanoelectrospray tandem mass spectrometry. J. Chromatogr. A 1130, 238–245.

Wang, J.R., Zhang, H.Y., Yau, L.F., Mi, J.N., Lee, S., Lee, K.C., Hu, P., Liu, L., Jiang, Z.H., 2014. Improved sphingolipidomic approach based on ultra-high performance liquid chromatography and multiple mass spectrometries with application to cellular neurotoxicity. Anal. Chem. 86, 5688–5696.

Wang, Y., Sun, S., Zhu, J., Cui, L., Zhang, H.L., 2015. Biomarkers of guillain-barre syndrome: some recent progress, more still to be explored. Mediators Inflamm. 2015, 12.

Weishaupt, N., Caughlin, S., Yeung, K.K., Whitehead, S.N., 2015. Differential anatomical expression of ganglioside gm1 species containing d18:1 or d20:1 sphingosine detected by maldi imaging mass spectrometry in mature rat brain. Front. Neuroanat. 9, 155.

Yamazaki, Y., Horibata, Y., Nagatsuka, Y., Hirabayashi, Y., Hashikawa, T., 2007. Fucoganglioside alpha-fucosyl(alpha-galactosyl)-gm1: a novel member of lipid membrane microdomain components involved in pc12 cell neuritogenesis. Biochem. J. 407, 31–40.

Yanagisawa, K., 2007. Role of gangliosides in alzheimer's disease. Biochim. Biophys. Acta 1768, 1943–1951.

Yanagisawa, M., Ariga, T., Yu, R.K., 2006. Fucosyl-gm1 expression and amyloid-β protein accumulation in pc12 cells. J. Neurosci. Res. 84, 1343–1349.

Yu, R.K., Nakatani, Y., Yanagisawa, M., 2009. The role of glycosphingolipid metabolism in the developing brain. J. Lipid Res. 50 (Suppl), S440–5.

Yu, R.K., Tsai, Y.T., Ariga, T., Yanagisawa, M., 2011. Structures, biosynthesis, and functions of gangliosides–an overview. J. Oleo Sci. 60, 537–544.

Zamfir, A.D., 2014. Neurological analyses: focus on gangliosides and mass spectrometry. Adv. Mass Spectrom. Biomed. Res. 806, 153–204.

Zhang, J., Ren, Y., Huang, B., Tao, B., Pedersen, M.R., Li, D., 2012. Determination of disialoganglioside gd3 and monosialoganglioside gm3 in infant formulas and whey protein concentrates by ultra-performance liquid chromatography/electrospray ionization tandem mass spectrometry. J. Sep. Sci. 35, 937–946.